Program Digest, 2019 IEEE International Ultrasonics Symposium (IUS)
Glasgow, Scotland, October 6-9, 2019

Ultrasonic mapping of endogenous motion in brain tissue

1st Monika Makūnaitė
Biomedical Engineering Institute
Kaunas University of Technology
Kaunas, Lithuania
monika.makunaite@ktu.edu

2nd Rytis Jurkonis
Biomedical Engineering Institute
Kaunas University of Technology
Kaunas, Lithuania
rytis.jurkonis@ktu.lt

3rd Vaidas Matijošaitis
Department of Neurology
Lithuanian University of Health Sciences
Kaunas, Lithuania
vaidas.matijosaitis@kaunoklinikos.lt

4th Daiva Rastenytė
Department of Neurology
Lithuanian University of Health Sciences
Kaunas, Lithuania
daiva.rastenyte@kaunoklinikos.lt

***Abstract*—Tissue pulsatility imaging is introduced as non-invasive ultrasonic (US) technique used to access endogenous motion of human brain. Increasing evidence suggests that brain tissue pulsatility have a potential to be used for diagnosis of neurodegenerative diseases. In this work, we aimed to assess quantitatively the brain tissue displacements with presented radiofrequency (RF) ultrasonic method. The obtained maps of intra-subject repeatable brain displacements enable spatial differentiation of dynamic structures from relatively static. Averaged displacement waveform in brain region were noticed to be intra-subject repeatable. The brain movement strength and mean frequency in mid-brain and hippocampus are explored in pilot groups of healthy volunteers and Alzheimer patients.**

Keywords—transcranial sonography, radiofrequency ultrasound, intra-subject repeatable waveform, motion mapping

I. INTRODUCTION

Tissue pulsatility imaging is introduced as non-invasive ultrasonic (US) technique used to access endogenous motion of human brain [1, 2]. Historically endogenous displacements in the brain were considered researching intra-cellular recordings in animals [3]. The arteries endogenously drive the animal brain tissue to pulsate more than a hundred micrometers. Few micrometers brain displacements corresponding to cardiac pulse were detected with implants [4] in small animal. With laser speckle contrast imaging cardiac pulsatility is mapped on the brain of a mouse [5]. Increasing evidence [2, 6, 7] suggests that brain tissue pulsatility have a potential to be used for diagnosis of neurodegenerative diseases.

Purpose of this work is to assess quantitatively the brain tissue displacements with autocorrelation based radiofrequency (RF) ultrasonic method. The presented assessment is specific to intra-subject repeated waveforms of intracranial movements.

II. MATERIALS AND METHODS

A. Data Acquisition

Transcranial acquisition was performed with US scanner Sonix Touch (Analogic Ultrasound, Canada) equipped with SA4-2 phased array transducer. The main parameters of transducer and data acquisition were as follows: 64 elements phased array transducer, angle of sector 60°, frequency of US waves 2.5 MHz, number of post-beamformed scanning lines 131, scanning depth 11 cm, frame rate 45 Hz, sampling frequency 40 MHz, ADC resolution 16 bits. RF US signals and B-mode images with outlined region of hippocampus and mid-brain were acquired and stored for off-line analysis.

Echoscopy was performed through the right and left temporal bones, with the scan plane positioned in horizontal (for mid-brain scan) and coronal (for hippocampus scan) planes of the skull. Both, transducer's and subject's head holders were implemented during sonography in order to reduce external movements. Subjects were scanned in the supine position, after instruction to keep the body motionless.

US data was collected from 20 healthy volunteers (HV) and 21 patients with Alzheimer disease (AD). Neurosonographer outlined the structures by hand on B-scan images. For cases of HV group the average range of hippocampus locations were 37 – 60 mm (average area 3.1 cm^2) and for mid-brain 63 – 92 mm (6.4 cm^2). For cases of AD group the average range of hippocampus locations were 37 – 59 mm (average area 2.9 cm^2) and for mid-brain 62 – 91 mm (6.1 cm^2). Area selection border was drawn by hand.

The study was approved by Kaunas Region Biomedical Research Ethics Committee (2017-12-19, No. BE-2-728, Kaunas, Lithuania). Every participant provided a written consent to participate in the study and allowed the usage of the obtained B-scan images and RF signals under the principle of confidentiality.

B. RF Ultrasound Signals Processing Algorithm used for Motion Detection

The motion of the brain tissue was detected selecting by every 600 points along the beam RF line in the region of interest (ROI), see Fig. 1A. These points' coordinates were used as the beginning of RF signal segments, see Fig. 1B. The motion along the beam line was estimated using cross-correlation function, calculated between obtained RF signal segments, and parabolic interpolation [8] of the peak of the correlation function. Motion signals in hippocampus and mid-brain regions were ROI-averaged from each side of scanning.

Cross-correlation lag between the segments at adjacent scanning frames k and $k + 1$ represents the inter-frame estimate of motion magnitude. The peak of the cross-correlation function was estimated as follows:

This work was funded by Research Council of Lithuania in the frame of Researchers group project "Radiofrequency Ultrasound-based Brain Tissue Assessment Method for the Diagnostics of Early Neurodegeneration (NeuroRD)" Reg. No.: MIP-17-457.

$$C_k[n] = \max_{-T \le z \le T} \left[\Im^{-1} \{ \Im[w[z] \cdot D_k^*[z]] \cdot \Im[w[z] \cdot D_{k+1}[z]] \} \right], \quad (1)$$

where D – RF signal segment at a certain scanning line and scanning depth, $\Im$ – fast Fourier transform, frame number $k = 1...K$, * – asterisk denotes complex conjugate. The empirical threshold value T was set at ± 150 μm, w – Hamming window function, $z = 1...Z$, Z – number of samples of RF signal segment (1.85 mm or six periods of US wave) used for the assessment of motion, n – correlation lag at the peak of the function The threshold T was used as a prevention of false peaks, which occur when a secondary correlation peak exceeds the primary peak.

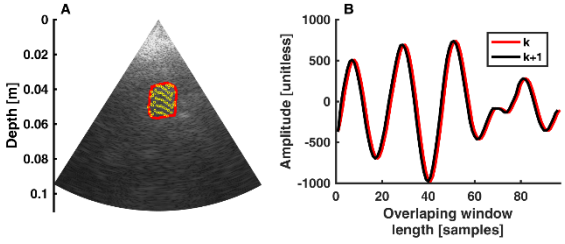

Fig. 1. B-scan image together with outlined cross-section of hippocampus (red line) and automatically selected every 600 points along the beam RF lines in ROI (A), RF signal segments of adjacent frames k and $k+1$ (B).

Because the estimated inter-frame motion had integer accuracy, parabolic interpolation [8] of the correlation peak was applied to achieve sub-sample resolution of the inter-frame motion estimates. The peak-shift estimate of the inter-frame motion $m_{IF}[k]$ was defined as follows:

$$m_{IF}[k] = \Delta d \cdot \left(\frac{C_k[n-1] - C_k[n+1]}{2 \cdot (C_k[n-1] - 2 \cdot C_k[n] + C_k[n+1])} + c_k[n] \right), \quad (2)$$

where $C_k[n-1]$ and $C_k[n+1]$ – nearest neighbours of the peak of cross-correlation function ($C_k[n]$), Δd –sampling period ($\Delta d = 19.25\ \mu m$), k –frame number ($k = 1...K$). The inter-frame motion signals obtained in the ROI were averaged in respect of space. The ROI-averaged inter-frame motion signal was expressed as follows:

$$\overline{m_{IF}[k]} = \frac{1}{p} \cdot \sum_{p=1}^{P} m_{IFp}[k], \quad (3)$$

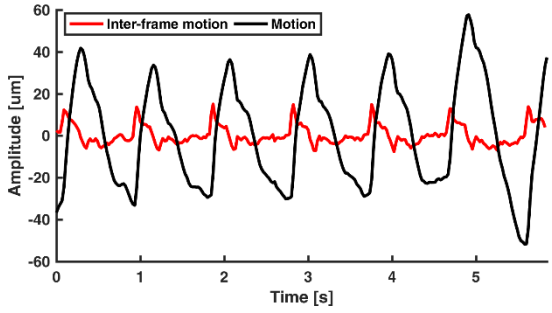

Fig. 2. The ROI-averaged inter-frame motion signal (red) and ROI-averaged motion signal (black) in mid-brain region.

where $p = 1...P$, P – number of points in ROI, $m_{IFp}[k]$ – inter-frame motion signal at p-th position in ROI. In order to get ROI-averaged motion signal $m[k]$, integral of ROI-averaged inter-frame motion signal $\overline{m_{IF}[k]}$ was calculated, see Fig. 2. Finally, the obtained ROI-averaged motion signal was high-pass filtered (cut-off frequency = 0.75 Hz) in order to focus on motions related to heart rate and to filter out slow movements arising due to respiration.

C. Algorithm for Motion Signal Periodicity Estimation

In the second stage of the algorithm, the intra-subject periodicity of ROI-averaged motion signal was used in order to reject possible artefacts of external motion. The ROI-averaged motion signal $m[k]$ was divided into Q waveforms. The similar Q waveforms were detected by using reference-template matching technique. Firstly, the reference waveform was manually selected observing the signal. The waveforms similar to the reference waveform were automatically detected using normalized cross-correlation function. The waveforms were assumed comparable if the normalized correlation coefficient value exceeded 0.7 [9]. The example of the ROI-average motion signal of mid-brain and the reference waveform is presented in Fig. 3A. Detected six ($Q=6$) similar waveforms of motion signal are marked by red colour. Fig. 3B shows averaged motion waveform $s_q[l]$ in respect of time of ROI-average motion signal. The averaged motion waveform was windowed by Tukey function before taking fast Fourier transform. Amplitude spectra of averaged motion waveform was obtained as follows:

$$S_q(f) = \Im \left[w_T[l] \cdot s_q[l] \right], \quad (4)$$

where L – length of averaged motion waveform ($l=1...L$), w_T– Hamming window function, $s_q[l]$ – averaged motion waveform, $S_q(f)$ – amplitude spectra of averaged motion waveform. Fig. 3C represents the amplitude spectra of the averaged motion waveform.

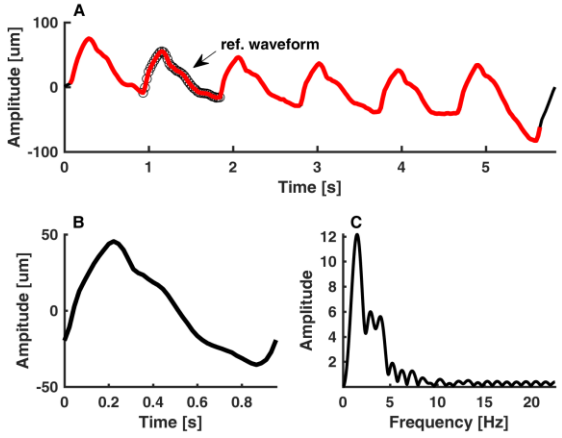

Fig. 3. Parametrisation of detected motion in ROI: ROI-averaged motion signal, manually selected intra-subject reference waveform and automatically detected similar $Q=6$ waveforms (A), intra-subject averaged waveform of motion (B), amplitude spectra of motion (C).

Finally, averaged motion waveform and spectrum of averaged motion waveform were parametrized by amplitude and mean frequency accordingly.

D. Motion Mapping

Motion map of the brain tissue in scanning plane was produced using similar methodology as for motion estimation in

ROI. The difference is that motion was estimated selecting by every 50 points along the beam line in the main part of the B-scan size. Motion map was obtained in the range from 27 mm to 104 mm according to depth and from 3rd to 128th according to echoscopic line. The inter-frame motion signals obtained in the B-scan were not averaged in respect of space. Only this step of the whole algorithm was skipped. After inter-frame motion signals were detected in the automatically preselected points, integration and periodicity estimation was done. If the motion signal had more than one similar motion waveform (reference waveform $+Q$ waveforms), the amplitude of the averaged motion waveform was determined. Otherwise, the amplitude of the averaged motion waveform was considered as zero.

III. Results

A total of US RF data of 41 participants (21 subjects with AD, and 20 HV) were involved in this study. In our method, we were assessing ROI-average motion signals that found intra-subject repeatable, see Fig. 4. A large variety of motion signals was observed in the mid-brain region.

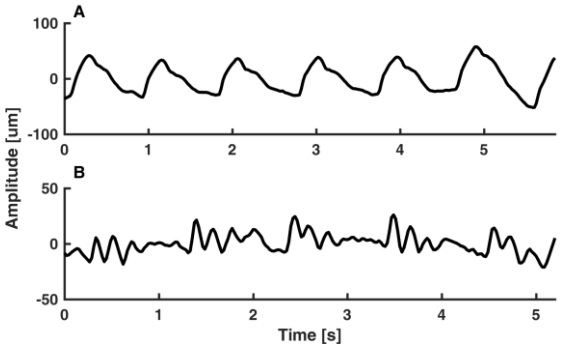

Fig. 4. Variability of waveforms of ROI-averaged motion signals in mid brain region. of HV group: mean frequency 3.9 Hz (A), mean frequency 5.6 Hz.

Magnitude estimates of endogenous displacements in the brain are comparable with estimates of others [10]. The slow drift of baseline in calculated displacement signals could be related to the breathing of the subject [11]. The mean frequency calculated from amplitude spectra represent which higher or lower frequency is dominant. Peculiarities of displacement amplitudes in a group of HV subjects' vs AD patients are present in the form of boxplots, see Fig. 5. We found that hippocampus regions in AD group vs HV show higher displacement amplitudes. This feature is observed from both sides of the cranium. Except for right mid-brain in AD group the displacements of structures are stronger than displacements HV structures. Peculiarities of dominant frequency of displacements are present in the form of boxplots, see Fig. 6. Displacements of AD hippocampus structures have a higher dominant frequency vs dominant frequency of HV hippocampus displacements.

We mapped amplitude estimates of displacement signals on coordinate grid of B-scan. The map represents displacement intensity in the main part of the plane of the scanning (see Fig. 7). The specifics of assessment is in considering the only intra-subject repeatable waveforms of displacements. This means that the motion amplitude is averaged from two or more repeated waveforms and coded in colour scale (from light blue to dark red). The non-repeated (or noise corrupted) motion signals were assigned as zero and depicted as dark blue colour areas in motion maps.

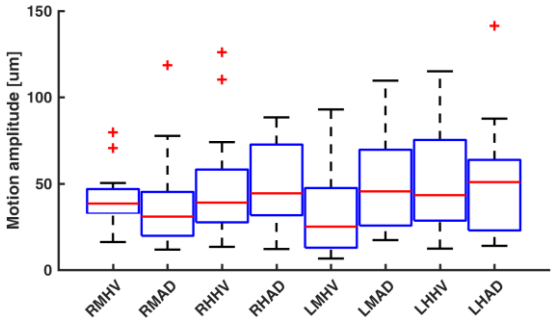

Fig. 5. Box-and-whiskers plot of motion amplitudes in different brain structures of HV groups and AD (successively n = 14, 16, 18, 18, 13, 17, 11, 15). Abbreviations: right midbrain (RM), left midbrain (LM), right hippocampus (RH), left hippocampus (LH), index HV represent healthy volunteers group, AD – Alzheimer disease.

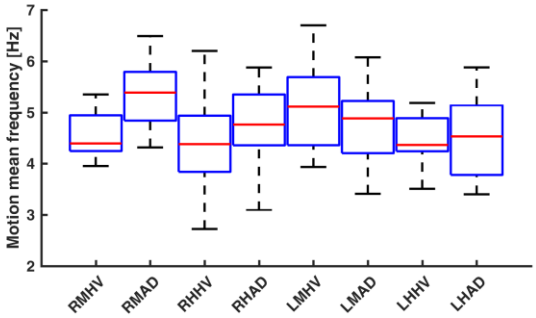

Fig. 6. Box-and-whiskers plot of motion mean frequency in different brain structures of HV groups and AD (successively n = 14, 16, 18, 18, 13, 17, 11, 15). Abbreviations: right midbrain (RM), left midbrain (LM), right hippocampus (RH), left hippocampus (LH), index HV represent healthy volunteers group, AD – Alzheimer disease.

IV. Discussion

The US method of brain displacements detection is evaluated with the RF data set of pilot groups of HV and AD participants. Mid-brain and hippocampus regions averaged estimates of tissue movements are obtained as intra-subject repeatable waveforms of endogenous pulsing. The region averaged and intra-subject repeatable displacement signals are quantified with help of magnitude and frequency estimates. Also, the magnitude of intra-subject repeatable displacements is mapped on the B-scan image grid. These motion maps could be used to differentiate dynamic brain tissue regions from relatively static structures. The statistics of region averaged displacements is inconclusive for separation of investigated groups. The dedicated quantification methods of findings in displacements maps are planned in future research.

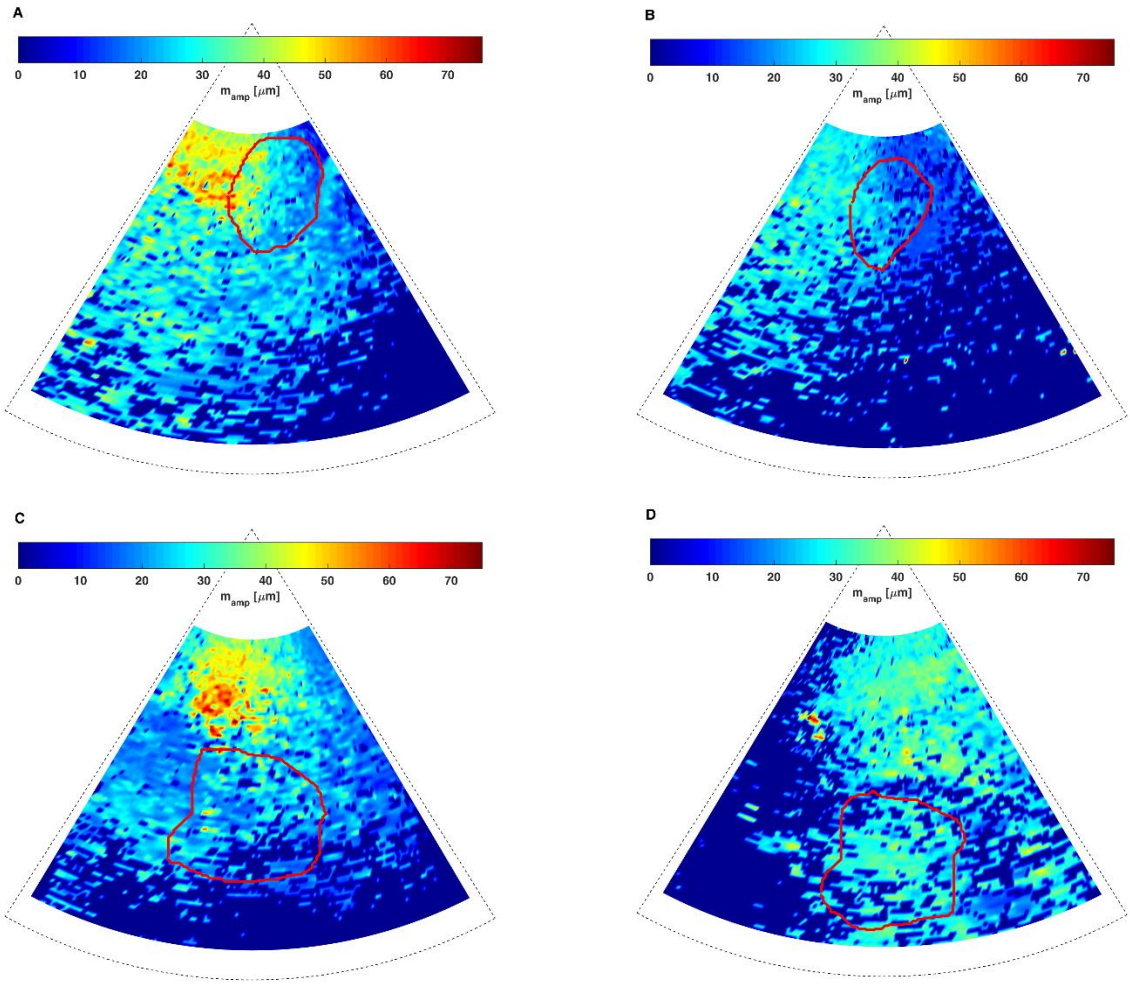

Fig. 7. Motion maps of brain tissue: coronal plane of healthy volunteer with outlined hippocampus region (A), coronal plane of patient with Alzheimer desease and outlined hippocampus region (B), horizontal plane of healthy volunteer with outlined mid-brain region (C), horizontal plane of patient with Alzheimer desease and outlined mid-brain region (D).

ACKNOWLEDGMENT

This work was funded by Research Council of Lithuania in the frame of Researchers group project "Radiofrequency Ultrasound-based Brain Tissue Assessment Method for the Diagnostics of Early Neurodegeneration (NeuroRD)" Reg. No.: MIP-17-457.

REFERENCES

[1] Kucewicz JC, Dunmire B, Leotta DF, Panagiotides H, Paun M, Beach KW. Functional tissue pulsatility imaging of the brain during visual stimulation. Ultrasound Med Biol 2007; 33 :681-690.

[2] Desmidt T, Brizard B, Dujardin P, et al. Brain tissue pulsatility is increased in midlife depression: A comparative study using ultrasound tissue pulsatility imaging. Neuropsychopharmacology 2017**; 42** :2575.

[3] R. H. Britt, G. T. Rossi, "Quantitative analysis of methods for reducing physiological brain pulsations," J Neurosci Meth, vol. 6, pp. 219-29., 1982.

[4] M. Polanco, S. Bawab. And H. Yoon "Computational Assessment of Neural Probe and Brain Tissue Interface under Transient Motion" Biosensors 2016, 6(2), 27;

[5] D. D. Postnov, S. E. Erdener, K. Kilic, and D. A. Boas, "Cardiac pulsatility mapping and vessel type identification using laser speckle contrast imaging," Biomed. Opt. Express 9, 6388-6397 (2018)

[6] Shirzadi Z, Robertson AD, Metcalfe AW, et al. Brain tissue pulsatility is related to clinical features of Parkinson's disease. NeuroImage: Clinical 2018; 20 :222-227.

[7] M. E. Wagshul, P. K. Eide, J. R. Madsen, "The pulsating brain: A review of experimental and clinical studies of intracranial pulsatility," Fluids Barriers CNS., vol. 8, no. 1, pp. 5-28, Jan. 2011,

[8] Céspedes I, Huang Y, Ophir J, Spratt S. Methods for estimation of subsample time delays of digitized echo signals. Ultrason Imaging 1995; 17 :142-171.

[9] J. P. Lewis. Fast Template Matching1995; 95 :120-123.

[10] R. Ternifi, X. Cazals, A. Lorette Thomas Desmidt, J.P. Remenieras "Correlation between Leukoaraiosis and natural brain tissue velocity: A pilot study using Ultrasound and MRI," 2012 IEEE International Ultrasonics Symposium, Dresden, 2012, pp. 945-948.

[11] D. Certon, R. Ternifi, A. Boulme, M. Legros, J.-G. Minonzio, M. Talmant, F. Patat, J.-P. Remenieras "Low frequency cMUT technology: Application to measurement of brain movement and assessment of bone quality" IRBM, Vol.34, Issue 2, 2013, pp 159-166